The determination of the thickness and the optical dispersion property of gold film using spectroscopy of a surface plasmon in the frequency domain*

Huang Yan(黄 妍), Ye Hong-An(叶红安)†, Li Song-Quan(李松权), and Dou Yin-Feng(窦寅丰)

School of Electronic Engineering, Heilongjiang University, Harbin 150080, *China*

(Received 11 July 2012; revised manuscript received 27 August 2012)

We propose to use wavelength modulation approach, i.e., the spectroscopy of a surface plasmon in the frequency domain, to characterize the optical dispersion property of gold film. Using this method, we determine the dispersion relationship of gold film in a wavelength range from 537.12 nm to 905.52 nm, and our results accord well with the reported results by other authors. This method is particularly suited for studying the optical dispersion properties of thin metal films, because a series of dielectric constants over a wide spectral range can be determined simultaneously via only a single scan of the incident angle, thereby avoiding the repeated measurements required when using the angular modulation approach.

Keywords: surface plasmon polaritons (SPPs), optical dispersion property, gold film

PACS: 73.20.Mf, 78.20.–e **DOI:** 10.1088/1674-1056/22/2/027301

1. Introduction

Surface plasmon polaritons (SPPs), also abbreviated as surface plasmons (SPs), present coupled electromagnetic field-collective charge density oscillations localized at the interface between a dielectric (with dielectric constant $\varepsilon_d > 0$) and a metal or semiconductor, of which the dielectric constant ($\varepsilon = \varepsilon_r + i\varepsilon_i$) has $\varepsilon_r < 0$. The surface plasmon resonance (SPR) phenomenon exhibits extremely high sensitivity to the optical and structural properties of the surface layer above the SP-supporting metal film. Owing to this feature, the SPR technique has been used in a wide range of applications including biosensing, drug development, food, safety, environmental monitoring, and medical diagnostics.[1–3] Especially, the SPR biosensor is the most advanced and developed optical label-free biosensor technology.[4]

As an important application, some earliest SPR studies were devoted to the determinations of the optical and geometrical constants of thin metal films, and so it has been confirmed that the SPR technique is an accurate and simple method of characterizing thin metal films,[5–16] and it is particularly suited for studying thin metal films of a few hundred angstroms in thickness.[5,17,18] In all studies of characterizing thin metal films using SPs, an attenuated total reflection (ATR) prism coupling in the Kretschmann–Raether geometry has been always employed as the method of optical excitation of SPs, and among the four modulation approaches (including modulations in wavelength, angle, amplitude, and phase), angular modulation is the only adopted approach. Generally, a one-layer model is employed to characterize thin metal films. When using a one-layer model, the metal films are considered to be homogeneous and perfectly flat[19] and each of them can be fully characterized by three parameters: the real part ε_r and imaginary part ε_i of the complex dielectric constant, and the thickness d. Evaluations of ε_r, ε_i, and d from experimental data points via curve-fitting method require to solve a set of nonlinear equations by using numerical procedure. For the convenience of calculation, it was proposed to model the SPR dip with Lorentzian curve. With this method ε_r, ε_i, and d can be evaluated simultaneously from three characteristic parameters of the SPR curve: the half-width $\Delta\theta_{1/2}$, the resonance angle θ_R, and the minimum reflectivity R_{min}.[5,20,21] However, modeling the reflectivity data by a Lorentzian curve leads to an ambiguity in the determination of the optical constants and the thicknesses of metal films.[5–8] The method of removing the ambiguity is to introduce an additional constraint by which thickness d can be uniquely determined, and then a unique solution of ε_r, ε_i, and d is obtained, such as by using the dual-wavelength method,[5,7] and the extended ATR spectrum.[20,22,23]

Real metal films cannot be perfectly flat, and the influence of surface/and interfaces roughness on an SPR curve has been studied extensively.[19,24–28] Investigations demonstrated that in the presence of surface roughness, the SPs are attenuated by two processes: radiation into the vacuum, or scattering into other surface-polariton states; and the former is responsible for increase in the resonant curve angular width, the latter leads to resonant curve shift.[28] Experiments also demonstrated that the effective dielectric functions and surface

*Project supported by the National Natural Science Foundation of China (Grant No. 61177079), the Open Fund of Key Laboratory of Electronics Engineering, College of Heilongjiang Province, China (Grant No. DZZD20100014), and the Youth Science Foundation of Heilongjiang University, China (Grant No. QL200914).

†Corresponding author. E-mail: yehonganhlj@gmail.com

© 2013 Chinese Physical Society and IOP Publishing Ltd

plasmon wavevectors of gold film change drastically under the influence of increasing roughness amplitude.[27] If we use a one-layer model to characterize metal films, we should know that the magnitude of the imaginary part of the dielectric constant from SPR measurement must be somewhat larger than that arising only from absorption process, because the attenuation of SPs due to plasmon scattering on surface roughness is not removed in calculating ε_i, and in consequence, the magnitude of the real part is smaller.[19] To describe the influence of the layers roughness, an intermediate layer accounting for the roughness at each interface was introduced in the model, and the optical property of the intermediate layer was modeled by the effective medium approximation.[19,25] To see how accurately the dielectric constants and thicknesses of metal films can be deduced from SP measurement, the influence of the layer roughness of an SP-supporting system (including the substrate, Cr film, and Au film) was thoroughly studied. In conclusion, the model with intermediate layer is more realistic and the results from this model are more reasonable. However, on the other hand, the one-layer model is much simpler and also good enough to describe the SP-supporting system by giving the effective dielectric functions. The model with intermediate layer is necessary only if we need to determine the dielectric constant which depends only on the internal structure of the metal film and is not influenced by its roughness.[19] Some experiments also demonstrated that the thicknesses obtained from SPR measurements using a one-layer model, coincide very well with those from the measurements by X-ray,[19] ellipsometry,[29] and atomic force microscopy (AFM).[20]

Until now, using SPs to determine optical constants and/or thickness of thin metal films still attracts considerable attention, which is, to a great extent, due to the requirements of developing the SPR technique itself. Thin metal films are an integral part of the SPR-based devices, such as the SPR sensors,[1,4] the metal-clad waveguide,[30–34] and the long-range SPP waveguide,[35–37] and the performances of these optical devices are determined dominantly by the optical and geometrical properties of the metal films. Furthermore, parameters of the overlayer (or overlayers) deposited above the metal films are often required to be determined correctly, and it is evident that the metal films must first be characterized accurately. In fact, the effective optical constants of the metal films also depend on their thickness, which is related to the internal structure, owing to the variation in film density and resistivity.[29,38–40]

For the development of sensors and other optical devices associated with SPR phenomenon, it is important to determine the dispersion properties for the most suitable metal films. Dispersion properties of silver and gold films have been studied using SPR technique with an angular modulation approach, and satisfactory results were obtained compared with the results obtained using other experimental methods and with the classical free electron model.[10,11,14] However, using the angular modulation approach to study the dispersion properties of metal films is intrinsically complex, because the measurement of the dielectric constants must be performed repeatedly at a series of sampled wavelengths. To simplify this tedious process, we propose to use the wavelength modulation approach, i.e., the spectroscopy of surface plasmon in the frequency domain to characterize the dispersion properties of the metal films. In our method, a well collimated broadband source is employed to excite the SPs with the construction of ATR prism coupling in the Kretschmann–Raether geometry. When the prism coated with SP-supporting film rotates step by step, a series of SPR curves in frequency domain are generated correspondingly, and each curve has its own minimum reflectivity and resonant wavelength which are then used to determine the dielectric constants at a series of wavelengths, and then the dispersion relationship of the metal film is obtained. This method is particularly convenient for studying the dispersion properties of thin metal films, because with only a single scan of the incident angle, a series of dielectric constants over a wide spectral range can be determined simultaneously, thereby avoiding the repeated measurements required when using the angular modulation approach. Using this method, we characterize the dispersion property of gold film in a wavelength range of 537.12 nm–905.52 nm, the obtained results accord well with those reported by other authors. To our knowledge, it is the first time that the wavelength modulation approach has been used to characterize the optical properties of metal films.

2. Experimental details

In order to investigate the optical dispersion property of gold film, we designed and built the measurement apparatus as shown in Fig. 1. A well collimated light beam from a broadband source (Tungsten halogen light source, AvaLight-Hal) is p-polarized by a Glan–Taylor polarizer, then utilized to excite the SPs. P-polarized light is coupled to the plasmon via a three-layer Kretschmann configuration consisting of prism-gold film-air (see Fig. 2). The reflected light from the SP-supporting system is monitored by an optic spectrometer (Ocean Optics USB4000), from which we can obtain the spectroscopy of surface plasmon in frequency domain. The prism (isosceles right-angled triangle) is mounted on a computer-controlled rotary stage to scan the angle of incidence. Gold film is coated on the face of right-angle side, and the face of hypotenuse acts as both the entrance face and the exit face (see Fig. 1). With this configuration, the light I_{out} output from the prism is always parallel to the incident light I_{in} during scanning the prism, which is very convenient for detection purposes.

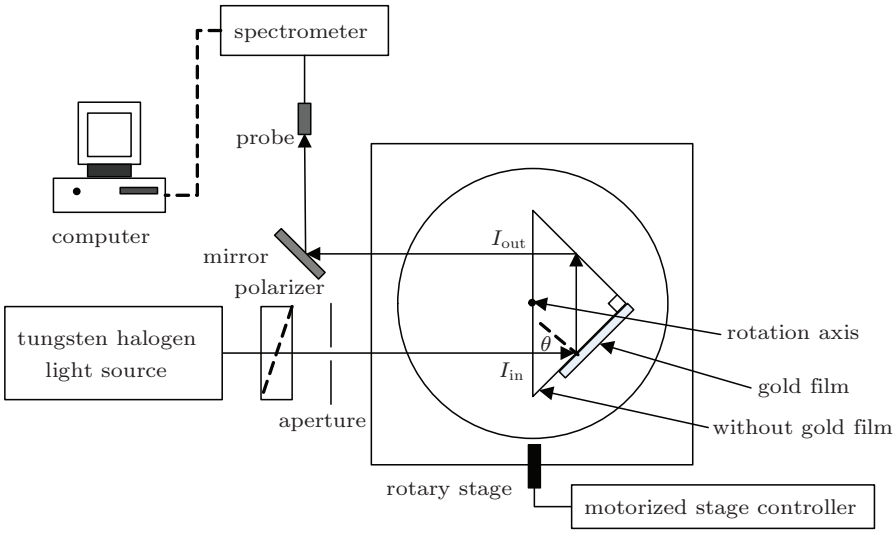


Fig. 1. Schematic diagram of the experimental apparatus for determination of the dispersion property of gold film.

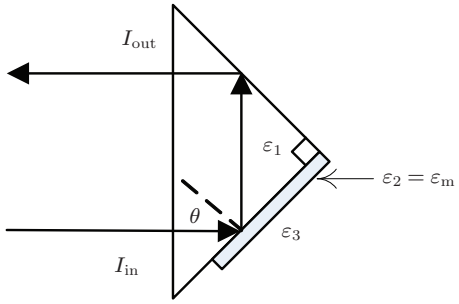


Fig. 2. Three-layer Kretschmann configuration.

Gold films are obtained by evaporating 99.999% pure gold onto a BK7 prism through electron-beam evaporation at a pressure of 6×10^{-3} Pa and room temperature. The evaporation rate is kept at about 0.2 nm/s and the thicknesses of prepared films are measured to be all 50 nm by using a quartz digital thickness monitor fixed inside the vacuum chamber. When scanning the angle of incidence through rotating the prism step by step, a series of SPR curves in the frequency domain are generated. Figure 3 shows the SPR curves of 50 sampled wavelengths (resonant wavelengths) in a wavelength range of 537.12 nm–905.52 nm, correspondingly the angular scanning range is $-4°$–$4.1°$ (against hypotenuse), and anticlockwise rotation is defined as being positive. The scanning step is 0.5° for a wavelength range of 537.12 nm–580.04 nm, and 0.1° for 580.04 nm–905.52 nm. To determine the absolute value of reflectivity of surface plasmon spectroscopy, the total internal reflection (TIR) spectrum of the light reflected from no-gold film part of the prism (see Fig. 1) is measured and taken as the calibration curve. The ratio between an SPR curve in Fig. 3 and the calibration curve gives the normalized SPR curve. Each normalized SPR curve has its own characteristic parameters: minimum reflectivity R_{min}, resonant wavelength λ_R, and incident angle θ_{spr} which are then utilized to determine the dielectric constant $\varepsilon_m(\lambda)$ at the relevant resonant wavelength. The experimental data should be corrected for reflections at the entrance and exit faces by considering both the angles of incidence against the faces and the dispersion effect of the prism.

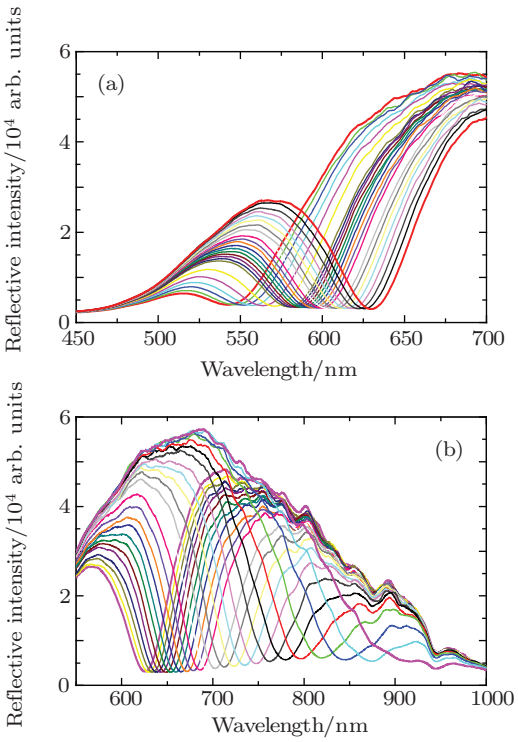


Fig. 3. (color online) SPR curves before calibration. (a) 25 SPR curves from $-4.0°$ to 1.6°. (b) 25 SPR curves from 1.6° to 4.1°.

As an example, the SPR curves before and after calibration at resonant wavelength $\lambda_R = 702.46$ nm are illustrated in Figs. 4(a) and 4(b), respectively. And Fig. 5 shows all of the 50 normalized SPR curves. From Fig. 4(b), we can clearly see the strong absorption peak at 484.60 nm which prohibits the ob-

taining of high-quality data below 537 nm, and beyond 905 nm the measurement is limited by the response of the spectrometer (responsive from 200 nm to 1100 nm) due to the degraded signal-to-noise ratio.

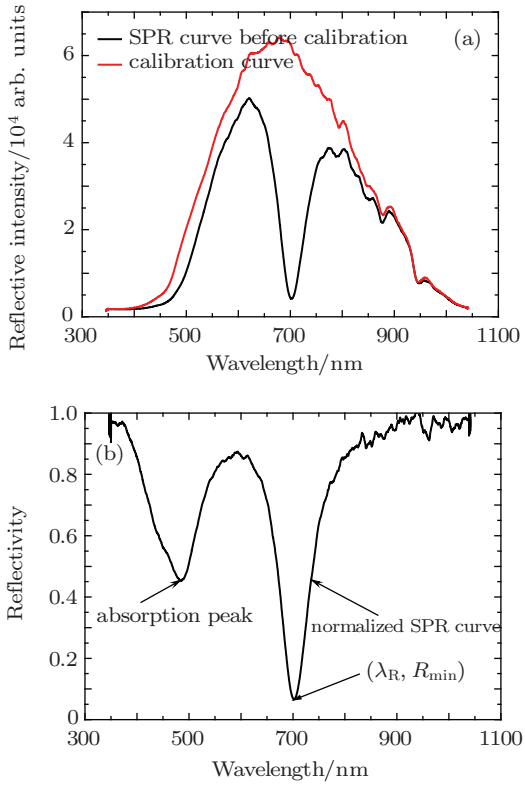


Fig. 4. (color online) SPR curves before and after calibration at $\lambda_R = 702.46$ nm. (a) The calibration curve and the SPR curve before calibration. (b) The SPR curve after calibration.

3. Theoretical analysis and results

The consideration presented here is restricted to an idealized metal film, i.e., one-layer model is used for characterizing the gold film. According to Fresnel's equations, the reflectivity R of p-polarization from the three-layer of Kretschmann's SPR configuration as shown in Fig. 2 can be expressed as

$$R = \left|r_{123}^{\mathrm{p}}\right|^2 = \left|\frac{r_{12}^{\mathrm{p}} + r_{23}^{\mathrm{p}} \exp\left(2\mathrm{i}k_{z2}d\right)}{1 + r_{12}^{\mathrm{p}} r_{23}^{\mathrm{p}} \exp\left(2\mathrm{i}k_{z2}d\right)}\right|^2, \tag{1}$$

$$r_{ij}^{\mathrm{p}} = \frac{\dfrac{k_{zi}}{\varepsilon_{\mathrm{i}}(\lambda)} - \dfrac{k_{zj}}{\varepsilon_j(\lambda)}}{\dfrac{k_{zi}}{\varepsilon_{\mathrm{i}}(\lambda)} + \dfrac{k_{zj}}{\varepsilon_j(\lambda)}}, \tag{2}$$

$$k_{zi(j)} = k_0[\varepsilon_{i(j)}(\lambda) - \varepsilon_1(\lambda)\sin^2\theta]^{1/2}, \tag{3}$$

where r_{ij}^{p} is the reflective coefficient at the boundary between i medium and j medium ($i, j = 1, 2, 3$), d represents the thickness of gold film, $k_{zi(j)}$ is the component of the wave vector in medium $i(j)$ in the z direction, $\varepsilon_1(\lambda)$, $\varepsilon_2(\lambda) = \varepsilon_{\mathrm{m}}(\lambda) = \varepsilon_{\mathrm{r}}(\lambda) + \mathrm{i}\varepsilon_{\mathrm{i}}(\lambda)$, and $\varepsilon_3(\lambda)$ are optical constants of prism, gold film, and air, respectively, k_0 is the wave vector in vacuum, and θ is the incident angle at the interface. In our discussion, the dispersion of air is ignored. To determine the incident angle θ correctly, the dispersion of the prism should be taken into account when the light is refracted on the entrance face.

We can proceed to determine the dispersion relationship and thickness of the gold film from the normalized SPR curves in Fig. 5. The dielectric constants corresponding to the 50 resonant wavelengths can be determined by the best fitting of the data, with R given by Eqs. (1)–(4) using the method of differential correction and iteration. In calculation by iteration, $\varepsilon_{\mathrm{r}}(\lambda)$, $\varepsilon_{\mathrm{i}}(\lambda)$, and d are taken as adjustable parameters, these parameters and dispersion relationship are evaluated through the following three steps.

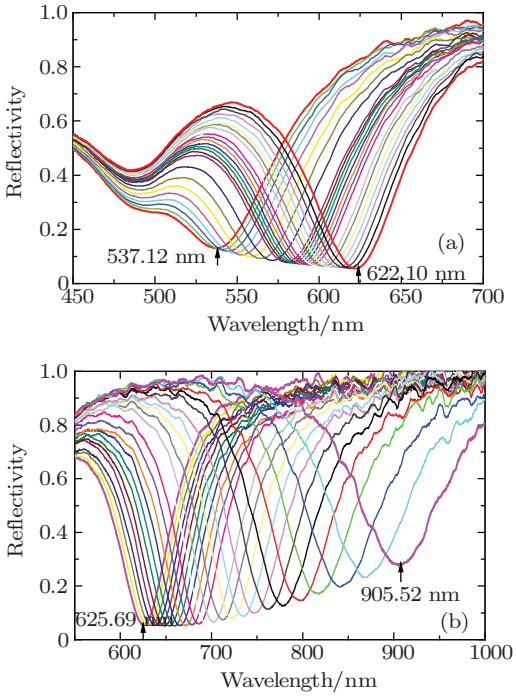


Fig. 5. (color online) The 50 normalized SPR curves covering a wavelength range of 537.12 nm–905.52 nm. (a) 25 SPR curves from 537.12 nm to 622.10 nm. (b) 25 SPR curves from 625.69 nm to 905.52 nm.

(I) Determine the possible range of d and the adjusted step Δd in iteration process. The value of d measured by quartz thickness monitor is 50 nm, thereby, (50±5) nm is a reasonable thickness range (to our experience). The adjusted step Δd in the iteration process is chosen as 0.1 nm, which is small enough because the influences on dielectric constant are all on the order of 10^{-4} for both $\Delta d = 0.1$ nm and $\Delta d = 0.01$ nm.

(II) Determine the initial values of $\varepsilon_{\mathrm{r}}(\lambda)$, and $\varepsilon_{\mathrm{i}}(\lambda)$ which will be used in stage (III) for each of the 50 resonant wavelengths by using the method of iteration. When thickness d is adjusted from 45 nm to 55 nm with $\Delta d = 0.1$ nm, 100 initial values of both $\varepsilon_{\mathrm{r}}(\lambda)$ and $\varepsilon_{\mathrm{i}}(\lambda)$ (corresponding to 100 values of thickness) for each of the 50 resonant wavelengths are evaluated by substituting θ_{spr} and the measured λ_{R} into Eqs. (1)–(4) and using the criterion function $R_{\min}^0[\varepsilon_{\mathrm{r}}(\lambda), \varepsilon_{\mathrm{i}}(\lambda)] - R_{\min} = 0$, where $R_{\min}^0$ and $R_{\min}$ repre-

sent the minimum reflectivities of theoretical and experimental SPR curve, respectively. And 100 dispersion curves are then established by using the above calculated initial values of $\varepsilon_r(\lambda)$ and $\varepsilon_i(\lambda)$ (for all the 50 resonant wavelengths) via the curve-fitting method.

(III) Determine the dispersion relationship and thickness of the gold film by using the 100 dispersion curves obtained from stage (II) via the method of differential correction. Assuming x to be a set of the model parameters ($\varepsilon_r(\lambda)$, $\varepsilon_i(\lambda)$, and d), the best fit is determined by computing the minimization of the objective function $F(x)$, which is defined as

$$F(x) = \sqrt{\frac{\sum_i^N \left[R_i^0(x) - R_i\right]^2}{N}}. \quad (4)$$

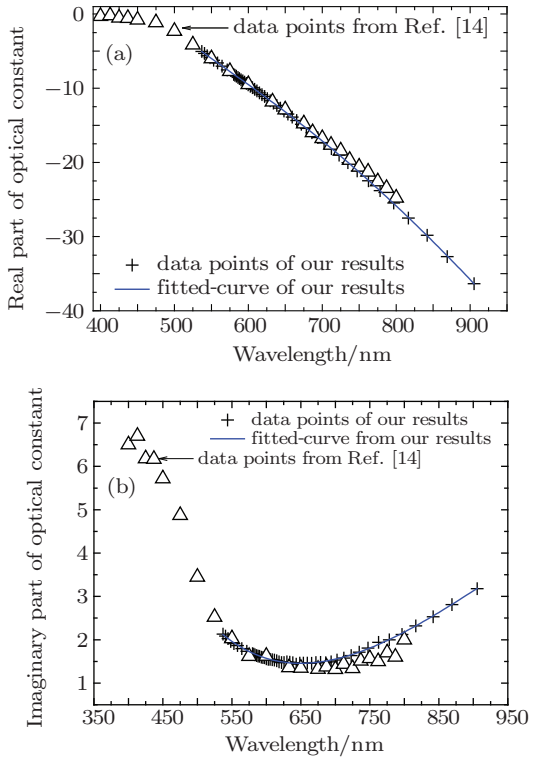


Fig. 6. Comparison of our results with those from Ref. [14]. (a) Real part of optical constants. (b) Imaginary part of optical constants.

Here $R_i^0(x)$ is the theoretical reflectivity computed by using the fitted dispersion curves from stage (II) and Eqs. (1)–(4), and R_i is the experimental reflectivity, i is a subscript for each of the N data points. In calculations, 200 data points near SPR dip are sampled for each of the 50 SPR curves, so here $N = 200$. In differential correction performance, we can find that there is only one dispersion curve (among the 100 dispersion curves) which makes $F(x)$ minimized. Just using this dispersion curve and Eqs. (1) to (3), a theoretical SPR curve near the dip (with its own resonant wavelength λ_R^0 and minimum reflectivity R_{min}^0) can be plotted. Using λ_R and the relevant dispersion curve, we can determine the values of $\varepsilon_r(\lambda)$, $\varepsilon_i(\lambda)$, and d, the results are listed in Table 1. The dispersion relationships of $\varepsilon_r(\lambda)$ and $\varepsilon_i(\lambda)$ from 537.12 nm to 905.52 nm shown in Fig. 6 are obtained by using the 50 dielectric constants listed in Table 1. The dispersion curves are fitted with sixth-order polynomial, which coincides very well with all the experimental data points, with the correlation coefficients $R^2 = 0.999995$ for $\varepsilon_r(\lambda)$ and $R^2 = 0.999221$ for $\varepsilon_i(\lambda)$. And histogram of the measured values of thicknesses is illustrated in Fig. 7, showing a good consistency of the measured thicknesses.

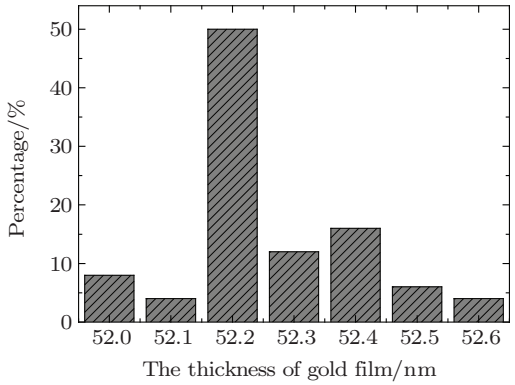


Fig. 7. Histogram of the measured values of thicknesses.

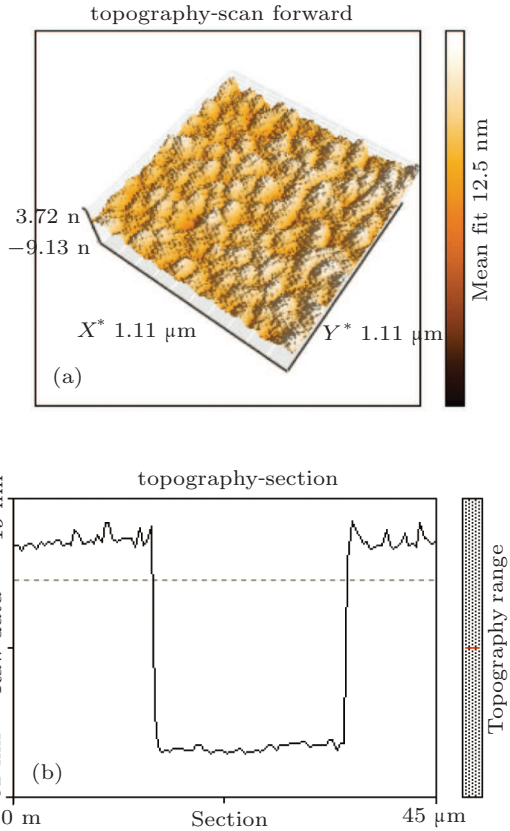


Fig. 8. (color online) AFM results of gold film deposited on the ATR prism. (a) Surface morphology. (b) Section analysis.

The thickness of the gold film is also measured by atomic force microscopy (Nanosurf Easyscan 2), the result $d = 52.31$ nm falls within the values determined from our measurements (see Fig. 8). From the property of the fitted disper-

sion curves and the consistency of the measured thicknesses, the validity of our method is further confirmed.

Table 1. Experimentally determined values of the real and imaginary parts ε_r and ε_i of the optical constants and thickness d of gold film using our method.

λ_R/nm	ε_r	$\Delta\varepsilon_r$	ε_i	$\Delta\varepsilon_i$	d/nm
537.12	–5.0540	±0.1104	2.1321	±0.0183	52.2
540.62	–5.3115	±0.0217	2.0832	±0.0166	52.2
544.32	–5.6222	±0.0202	2.0256	±0.0158	52.2
548.22	–5.8943	±0.0216	1.9623	±0.0126	52.2
552.93	–6.2310	±0.0644	1.9129	±0.0122	52.2
558.25	–6.5999	±0.0159	1.8652	±0.0113	52.2
564.38	–7.0288	±0.0161	1.7955	±0.0105	52.2
571.51	–7.5246	±0.0177	1.7345	±0.0097	52.2
580.04	–8.1350	±0.0162	1.6788	±0.0091	52.2
581.86	–8.2551	±0.0161	1.6693	±0.0090	52.2
583.69	–8.3912	±0.0162	1.6511	±0.0089	52.2
585.91	–8.5422	±0.0161	1.6359	±0.0088	52.2
587.94	–8.6867	±0.0160	1.6244	±0.0087	52.2
590.16	–8.8555	±0.0160	1.6193	±0.0087	52.2
592.58	–9.0106	±0.0160	1.5973	±0.0086	52.2
595.00	–9.1780	±0.0160	1.5883	±0.0085	52.2
597.42	–9.3474	±0.0161	1.5870	±0.0084	52.2
599.84	–9.5324	±0.0159	1.5627	±0.0082	52.4
602.66	–9.7275	±0.0159	1.5494	±0.0081	52.4
605.47	–9.9359	±0.0162	1.5499	±0.0082	52.2
608.49	–10.1434	±0.0160	1.5389	±0.0081	52.2
611.69	–10.3736	±0.0162	1.5337	±0.0080	52.2
614.90	–10.6176	±0.0162	1.5146	±0.0078	52.4
618.30	–10.8615	±0.0162	1.4894	±0.0078	52.3
622.10	–11.1181	±0.0163	1.4760	±0.0077	52.5
625.69	–11.3934	±0.0164	1.4743	±0.0076	52.4
629.67	–11.6857	±0.0164	1.4903	±0.0077	52.2
633.85	–12.0007	±0.0165	1.4820	±0.0076	52.2
638.42	–12.3257	±0.0167	1.4719	±0.0075	52.2
643.37	–12.6791	±0.0167	1.4385	±0.0072	52.5
648.32	–13.0670	±0.0169	1.4615	±0.0073	52.3
653.65	–13.4716	±0.0171	1.4613	±0.0072	52.3
659.36	–13.8972	±0.0172	1.4607	±0.0072	52.3
665.46	–14.3590	±0.0172	1.4556	±0.0072	52.4
671.73	–14.8586	±0.0174	1.4723	±0.0073	52.3
678.57	–15.4027	±0.0177	1.4776	±0.0073	52.4
685.98	–15.9873	±0.0177	1.4700	±0.0072	52.6
693.95	–16.6479	±0.0179	1.4906	±0.0073	52.6
702.46	–17.3636	±0.0181	1.5307	±0.0074	52.5
712.30	–18.1429	±0.0184	1.5757	±0.0075	52.4
722.86	–19.0284	±0.0184	1.6347	±0.0076	52.4
734.71	–20.0354	±0.0185	1.7141	±0.0078	52.2
747.25	–21.1368	±0.0187	1.8103	±0.0080	52.0
762.54	–22.4632	±0.0192	1.9404	±0.0082	52.0
778.29	–23.8133	±0.0594	1.9962	±0.0082	52.1
796.69	–25.4682	±0.0212	2.1214	±0.0085	52.2
816.59	–27.4998	±0.0489	2.3217	±0.0096	52.0
841.89	–29.8267	±0.0221	2.5298	±0.0094	52.1
869.00	–32.7075	±0.0231	2.8116	±0.0103	52.0
905.52	–36.3604	±0.0553	3.1787	±0.0119	52.3

In Fig. 6, we also plot other authors' data[14] for comparison. It is clearly seen that our results accord quite well with the results from Ref. [14]. The slight difference between these two results might arise from the difference in surface roughness amplitude between the two samples.

Now we discuss the resulting errors of $\varepsilon_r(\lambda)$ and $\varepsilon_i(\lambda)$ from our method. As mentioned above, we have determined the values of $\varepsilon_r(\lambda)$ and $\varepsilon_i(\lambda)$ by λ_R (corresponding to the experimental curves in Fig. 5), but there is a discrepancy between λ_R and the theoretical value of λ_R^0 obtained from the fitted SPR curve, also a discrepancy exists between R_{min} and R_{min}^0. Using $\Delta\lambda_R = \lambda_R - \lambda_R^0$, $\Delta R_{min} = R_{min} - R_{min}^0$, and the relevant dispersion curves of $\varepsilon_r(\lambda)$ and $\varepsilon_i(\lambda)$, we can estimate the measurement errors $\Delta\varepsilon_r$ and $\Delta\varepsilon_i$ arising from $\Delta\lambda_R$ and ΔR_{min}. Analysis demonstrates that (i) for $\varepsilon_r(\lambda)$ the influence of $\Delta\lambda_R$ is dominant (over 10^3 times larger than the influence of ΔR_{min}); (ii) for $\varepsilon_i(\lambda)$ the influence of ΔR_{min} is dominant (over 10 times larger than the influence of $\Delta\lambda_R$); (iii) $\Delta\lambda_R$ is almost the same as the readout resolution of the spectrometer (0.21 nm); (iv) ΔR_{min} is almost the same as the power stability of the light source (0.1%). From (i) to (iv), we can draw the conclusion that the measurement error $\Delta\varepsilon_r$ can be estimated by using the relevant dispersion curve of $\varepsilon_r(\lambda)$ under the assumption of $\Delta\lambda_R = \pm 0.21$ nm; $\Delta\varepsilon_i$ can be estimated by using the relevant dispersion curve of $\varepsilon_i(\lambda)$ under the assumption of $\Delta R_{min} = \pm 0.1\%$. The errors for the 50 dielectric constants are also listed in Table 1.

4. Conclusions

For the first time we propose to use the wavelength modulation approach, i.e., the spectroscopy of surface plasmon in frequency domain to characterize the dispersion properties of the metal films. The dispersion relationship of gold film in a wavelength range from 537.12 nm to 905.52 nm is determined, and the obtained results accord well with those from other authors. The validity of our method is also confirmed by the excellent coincidence between the fitted dispersion curves and all the experiments data points, and by the consistency of measured thicknesses. The thickness measured by using the wavelength modulation approach is in good agreement with that measured by AFM. This method is particularly suited for studying the optical dispersion properties of thin metal films, because a series of dielectric constants over a wide spectral range can be determined simultaneously via only a single scan of the incident angle, thereby avoiding the repeated measurements required when using the angular modulation approach.

References

[1] Navratilova I and Myszka D G 2006 *Surface Plasmon Resonance Based Sensors* (Berlin: Springer) pp. 155–160
[2] Hoa X D, Kirk A G and Tabrizian M 2007 *Biosens. Bioelectron.* **23** 151
[3] Homola J, Yee S S and Gauglitz G 1999 *Sens. Actuators* B **54** 3
[4] Piliarik M and Homola J 2009 *Opt. Express* **17** 16505
[5] Chen W P and Chen J M 1981 *J. Opt. Soc. Am.* **71** 189
[6] Yang F, Cao Z and Fang J 1988 *Appl. Opt.* **27** 11
[7] Robertson W M and Fullerton E 1989 *J. Opt. Soc. Am.* B **6** 1584
[8] De Bruijn H E, Kooyman R P H and Greve J 1990 *Appl. Opt.* **29** 1974
[9] Pokrowsky P 1991 *Appl. Opt.* **30** 3228

[10] Hsu T M, Chang C C, Hwang Y F and Lee K C 1983 *Chin. J. Phys.* **21** 26
[11] Gugger H, Jurich M and Swalen J D 1984 *Phys. Rev.* B **30** 4189
[12] Forstmann F and Stenschke H 1977 *Phys. Rev. Lett.* **38** 1365
[13] Borensztein Y 1983 *J. Opt. Soc. Am.* **73** 80
[14] Innes R A and Sambles J R 1987 *J. Phys.* F: *Met. Phys.* **17** 277
[15] Kretschmann E and Raether H 1968 *Z. Naturf.* A **23** 2135
[16] Otto A 1968 *Z. Phys.* **216** 398
[17] Abeles F 1965 *Optical Properties and Electronic Structure of Metals and Alloys* (Amsterdam: North-Holland) pp. 25–30
[18] Lopez-Rios T and Vuye G 1979 *Surf. Sci.* **81** 529
[19] Velinov T, Ahtapodov L, Nelson A, Gateshki M and Bivolarska M 2011 *Thin Solid Films* **519** 2093
[20] Rengevych O V, Shirshov Yu M, Ushenin Yu V and Beketov A G 1999 *Quantum Electron. & Optoelectronics* **2** 28
[21] Gu J H, Cao Z Q, Shen Q S and Chen G 2008 *J. Phys.* D: *Appl. Phys.* **41** 155309
[22] Levesque L 2011 *Opt. & Laser Technol.* **43** 14
[23] Cowen S and Sambles J R 1990 *Opt. Commun.* **79** 427
[24] Zhang S, Berguiga L, Elezgaray J, Roland T, Faivre-Moskalenko C and Argoul F 2007 *Surf. Sci.* **601** 5445
[25] Niklasson G V, Granqvist C G and Hunderi O 1981 *Appl. Opt.* **20** 26
[26] Burstein E, Chen W P, Chen Y J and Hartstein A 1974 *J. Vac. Sci. Technol.* **11** 1004
[27] Hoffmann A, Lenkefi Z and Szentirmay Z 1998 *J. Phys.: Condens. Matter* **10** 5503
[28] Mills D L 1975 *Phys. Rev.* B **12** 4036
[29] Wook-Jae L, Jae-Eun K, Hae Yong P, Suntak P, Min-Su K, Jin Tae K and Jung Jin J 2008 *J. Appl. Phys.* **103** 073713
[30] Harris R D and Wilkinson J S 1995 *Sens. Actuators* B **29** 261
[31] Zourob M, Mohr S, Brown B, Fielden P, McDonnell M and Goddard N 2003 *Sens. Actuators* B **90** 296
[32] Chen F, Cao Z, Shen Q, Deng X, Duan B, Yuan W, Sang M and Wang S 2005 *Opt. Express* **13** 10061
[33] Lu H, Cao Z, Li H, Shen Q and Deng X 2006 *Opt. Lett.* **31** 386
[34] Chen G, Cao Z, Gu J and Shen Q 2006 *Appl. Phys. Lett.* **89** 081120
[35] Nikolajsen T, Leosson K, Salakhutdinov I and Bozhevolnyi S I 2003 *Appl. Phys. Lett.* **82** 668
[36] Burke J J, Stegeman G I and Tamir T 1986 *Phys. Rev.* B **33** 5186
[37] Berini P 2000 *Phys. Rev.* B **61** 10484
[38] Yano M, Fukui M, Haragichi M and Shintani Y 1990 *Surf. Sci.* **227** 129
[39] Gadenne P and Vuye G 1997 *J. Phys.* E **10** 733
[40] Reale C 1970 *Infrared Phys.* **10** 173